



1 **Isotopic partitioning of nitrogen in PM_{2.5} at Beijing and a**
2 **background site of China**

3

4 Yan-Li Wang¹, Xue-Yan Liu^{2,3*}, Wei Song², Wen Yang¹, Bin Han¹, Xiao-Yan Dou⁴,

5 Xu-Dong Zhao⁴, Zhao-Liang Song^{2,3}, Cong-Qiang Liu^{2,3}, Zhi-Peng Bai^{1*}

6

7 ¹ State Key Laboratory of Environmental Criteria and Risk Assessment, Chinese Research

8 Academy of Environmental Sciences, Beijing, 100012, China

9 ² Institute of Surface-Earth System Science, Tianjin University, Tianjin, 300072, China

10 ³ State Key Laboratory of Environmental Geochemistry, Institute of Geochemistry, Chinese

11 Academy of Sciences, Guiyang, 550002, China

12 ⁴ Qinghai Environmental Monitoring Center, Xining, 810007, China

13

14

15 * Correspondence to:

16 Xue-Yan Liu and Zhi-Peng Bai

17 E-mails: liuxueyan@tju.edu.cn; baizp@craes.org.cn

18

19 Word count:

20 Abstract: 281

21 Text: 5343 (Introduction to Acknowledgments, Table and Figure captions)

22 2 Table, 4 Figures

23

24

25

26 **Abstract.**

27 Using isotope mixing model (IsoSource) and natural $\delta^{15}\text{N}$ method, this study
28 evaluated contributions of major sources to N of $\text{PM}_{2.5}$ at Beijing (collected during a
29 severe haze episode of January 22nd – 30th, 2013) and a background site (Menyuan,
30 Qinghai province; collected from September to October of 2013) of China. At Beijing,
31 $\delta^{15}\text{N}$ values of $\text{PM}_{2.5}$ (-4.1 – +13.5‰; mean = +2.8 ± 6.4‰) distributed within the
32 range reported for major anthropogenic sources (including NH_3 and NO_2 from coal
33 combustion, vehicle exhausts and domestic wastes/sewage). However, $\delta^{15}\text{N}$ values of
34 $\text{PM}_{2.5}$ at the background site (+8.0 – +27.9‰; mean = +18.5 ± 5.8‰) were
35 significantly higher than that of potential sources (including NH_3 and NO_2 from
36 biomass burning, animal wastes, soil N cycle, fertilizer application, and organic N of
37 soil dust). Evidences from molecular ratios of NH_4^+ to NO_3^- and/or SO_4^{2-} in $\text{PM}_{2.5}$,
38 NH_3 to NO_2 and/or SO_2 in ambient atmosphere suggested that the equilibrium of
39 $\text{NH}_3 \leftrightarrow \text{NH}_4^+$ caused apparent ^{15}N enrichment only in NH_4^+ of $\text{PM}_{2.5}$ at the background
40 site due to more abundant NH_3 than SO_2 and NO_2 . Therefore, a net ^{15}N enrichment
41 (33‰) was assumed for NH_3 sources of background $\text{PM}_{2.5}$ when fractional
42 contributions were estimated by IsoSource model. Results showed that 41%, 30% and
43 14% of N in $\text{PM}_{2.5}$ of Beijing originated from coal combustion, vehicle exhausts and
44 domestic wastes/sewage, respectively. Background $\text{PM}_{2.5}$ derived N mainly from
45 biomass burning (58%), animal wastes (15%) and fertilizer application (9%). These
46 results revealed the regulation of the stoichiometry between ammonia and acidic
47 gases on $\delta^{15}\text{N}$ signals in $\text{PM}_{2.5}$. Emissions of NO_2 from coal combustion and NH_3
48 from urban transportation should be strictly controlled to advert the risk of haze
49 episodes in Beijing.

50



51 1 Introduction

52 Over the past two decades, increasing fine particulate matter (PM, such as PM_{2.5} with
53 an aerodynamic diameter less than 2.5 μm) pollution events as well as haze days have
54 been observed in many urbanized and populated areas of China (Zhang et al., 2013).
55 Recent source-apportionment studies suggested that prior regulations should be
56 planned on industrial and transport-related emissions (such as NH₃, NO₂, SO₂, etc)
57 with major sources from combustions of fossil fuels (Guo et al., 2014; Huang et al.,
58 2014). In parallel, studies showed substantial but uncharacterized contributions from
59 non-fossil emissions, particularly from agricultural and biogenic sources in rural
60 regions (Huang et al., 2014; Zhang et al., 2015). Deciphering origins of key
61 components (such as nitrogen (N) and sulfur (S)) in PM_{2.5} at Beijing and the
62 background site are needed for a better evaluation of anthropogenic precursor
63 emissions and efficient mitigation of PM pollution in China (Cheng et al., 2011; Fu et
64 al., 2015).

65 Nitrogen, a key component in aerosol formation and pollution, has been
66 concerned in almost all source-apportionment studies of PM_{2.5} (Zhang, 2010; Guo et
67 al., 2014). The N in atmospheric PM, especially secondary particles, is mainly
68 comprised of inorganic ions (i.e., nitrate (NO₃⁻) and ammonium (NH₄⁺)), with
69 relatively lower fractions of non-soluble N (e.g., accounting for ~3% of TN in TSP at
70 Jesu island) (Kundu et al., 2010). Nitrogen oxides (mainly NO₂) are major precursors
71 during the formation of both secondary inorganic (as NO₃⁻) and organic (as organic
72 NO₃⁻) aerosols (Huang et al., 2014). Ammonia (NH₃), the precursor of NH₄⁺, readily
73 reacts with available SO₂ and NO₂ to produce ammonium salts, which plays a key
74 role in the formation of inorganic aerosols and fine particles (Guo et al., 2014). It
75 should be noted that NH₃ can also be transformed to organic N or amines in the



76 atmosphere. In other words, NO_2 and NH_3 precursors could not be transformed into
77 corresponding inorganic ions completely (Ge et al., 2011ab). Moreover, contributions
78 of NO_2 and NH_3 to counter ions vary among PM with different aerodynamic
79 diameters. Hence it may not be straightforward to elucidate gaseous N sources using
80 inorganic N analyses in $\text{PM}_{2.5}$, or elucidate inorganic N in $\text{PM}_{2.5}$ based on ambient
81 NO_2 and NH_3 levels. Compared with the expensive and complex monitoring of
82 gaseous and particulate N compounds, the natural abundance of N isotope ($\delta^{15}\text{N}$: the
83 $^{15}\text{N}/^{14}\text{N}$ ratio expressed relative to atmospheric N_2) in $\text{PM}_{2.5}$ can integrate all-involved
84 N sources, as well as reflect potential $\delta^{15}\text{N}$ changes of major N components during the
85 formation of $\text{PM}_{2.5}$ (Heaton, 1986; Michalski et al., 2004; Kendall et al., 2007; Elliott
86 et al., 2007, 2009; Savarino et al., 2013). It calls for lower cost and less labor force
87 than tedious isotopic analyses of inorganic and organic N components. Besides, $\delta^{15}\text{N}$
88 of $\text{PM}_{2.5}$ has an advantage of characterizing sources of major N pollutants and
89 providing the $\delta^{15}\text{N}$ information of dry N deposition for biogeochemistry studies
90 (Yeatman et al., 2001; Heaton et al., 2004; Elliott et al., 2007, 2009). At remote sites,
91 $\delta^{15}\text{N}$ of $\text{PM}_{2.5}$ can show influences of non-point sources (e.g., agricultural N emissions)
92 on background atmospheric N chemistry. At polluted sites (e.g., during severe haze
93 episodes in urban areas), $\delta^{15}\text{N}$ of $\text{PM}_{2.5}$ can provide direct evidences on sources and
94 extents of anthropogenic N pollution.

95 The $\delta^{15}\text{N}$ variation of $\text{PM}_{2.5}$ is controlled by $\delta^{15}\text{N}$ values of initial gas precursors
96 and gas (g) \leftrightarrow particle (p) isotope effects. It is ideal but difficult to measure $\delta^{15}\text{N}$
97 values of each potential source at any given sites which might need a reasonably long
98 period. Some N sources had actually small regional or global variability in $\delta^{15}\text{N}$
99 values (Walters et al., 2015), but some others showed a wide but similar $\delta^{15}\text{N}$ ranges
100 at different locations (Hoering et al., 1957; Heaton, 1986, 1990; Ammann et al., 1999;



101 Pearson et al., 2000). Hence, the mean values of documented $\delta^{15}\text{N}$ values in
102 precursors and precipitation were often used when constraining sources and fates of N
103 in atmospheric and ecosystem processes (Kendall et al., 2007; Elliott et al., 2007,
104 2009; Kawashima et al., 2011; Michalski et al., 2014). At present, available studies
105 have virtually covered $\delta^{15}\text{N}$ values of dominant natural and anthropogenic sources of
106 $\text{PM}_{2.5}$ (Fig. 1) which were also stressed in emission inventory and
107 source-apportionment studies (Felix et al., 2013; Divers et al., 2014). During the
108 formation of primary and secondary aerosols, N (mainly as organic N) in soil dusts
109 constitutes a primary and common N source (Zhang, 2010; Huang et al., 2014). At
110 remote/background sites, if there was no substantial influence from the burning of
111 agricultural biomass and fertilizer application (assumed as the main agricultural N
112 sources in this study), the major N source for secondary inorganic aerosols is soil NO_2
113 emission, which is distinctly ^{15}N -depleted due to the large ^{15}N discriminations during
114 gaseous NO_2 losses of soil N cycle (Felix et al., 2014). $\text{PM}_{2.5}$ at background sites is
115 expected to have low $\delta^{15}\text{N}$ values when atmospheric reactive N is substantially
116 contributed from N emissions of agricultural fertilization and livestock, both of which
117 are strongly ^{15}N -depleted (Elliott et al., 2007; Felix et al., 2014). However, when the
118 inorganic N is dominated by N emissions from biomass burning (the other major
119 agricultural activity, especially in harvest seasons), the $\delta^{15}\text{N}$ values of $\text{PM}_{2.5}$ are
120 expected to be positive because biomass burning emits N with $\delta^{15}\text{N}$ values distinctly
121 higher than biogenic and other agricultural N sources (Kawashima et al., 2011; Divers
122 et al., 2014). At urban sites, sources of N in $\text{PM}_{2.5}$ are largely anthropogenic. In
123 summary, the $\delta^{15}\text{N}$ values are negative for NH_3 from urban wastes/sewage (Heaton et
124 al., 1986), industries and vehicles (Felix et al., 2013), but are exclusively positive for
125 NO_2 from coal-fired power plants (Felix et al., 2012). Vehicle exhaust NO_2 , a major



126 source of NO₂ in the urban, had a wide $\delta^{15}\text{N}$ range (-19.1 – +9.8‰; a mass-weighted
127 value: $-2.5 \pm 1.5\%$) (Walters et al., 2015) because of the kinetic isotope fractionations
128 associated with the catalytic NO₂ reduction.

129 Besides sources, isotope effects the association of emitted N gases with
130 atmospheric PM have long been poorly studied. In general, the net isotopic effects
131 were assumed to be mainly derived from NH₃, with very small gas-to-particle
132 fractionation for nonvolatile NO₂ because its reaction and conversion is less limited
133 by counter ions (Yeatman et al., 2001; Kawashima et al., 2011). The assumption was
134 supported by small difference in mean $\delta^{15}\text{N}$ values between roadside NO₂ (5.7‰) and
135 particulates (6.8‰) (Ammann et al., 1999; Pearson et al., 2000). For NH₃, kinetic
136 isotopic effect of NH₃-to-NH₄⁺ reaction was small at the whole time scale of PM
137 formation, but NH₃↔NH₄⁺ equilibrium will cause ¹⁴N to be preferentially associated
138 with NH₃ and ¹⁵N to be enriched in NH₄⁺ of PM due to the stronger associative
139 strength of ¹⁵N than ¹⁴N in NH₄⁺ (Heaton et al., 1997; Fukuzaki et al., 2009; Li et al.,
140 2012). This has been recognized as a major reason for generally higher $\delta^{15}\text{N}$ -NH₄⁺ in
141 aerosols than that in rain NH₄⁺ and precursor NH₃ (Yeatman et al., 2001a,b; Jia and
142 Cheng 2010; Felix et al., 2013). In a hypothetical model proposed by Heaton et al
143 (1997), the $\delta^{15}\text{N}$ of particulate NH₄⁺ stabilized at values of 33‰ higher than that of
144 NH₃ at 25 °C. However, chemical equilibrium mechanisms and isotopic effects for
145 NH₃↔NH₄⁺ exchange in PM_{2.5} and its environmental controls are still uncertain in the
146 field circumstances. It is valuable to explore $\delta^{15}\text{N}$ characteristics of PM_{2.5} and the
147 mechanisms behind the $\delta^{15}\text{N}$ difference between PM_{2.5} and precursor gases.

148 This study measured $\delta^{15}\text{N}$ ratios of PM_{2.5} at Beijing (CRAES site) and a national
149 atmospheric background monitoring station (Menyuan, Qinghai province,
150 northwestern China). Based on the $\delta^{15}\text{N}$ values of observed PM_{2.5} samples and



151 potential N sources, a stable isotopic mixing model (IsoSource; Phillips et al., 2003)
152 was used to calculate fractional contributions of major sources to TN in PM_{2.5}. The
153 main objective of this paper is to explore an isotopic regime for differentiating
154 specific sources of N in atmospheric PM_{2.5}. As inorganic N in the atmosphere was
155 dominated by NH₄-N at both sites, we hypothesized that significant ¹⁵N enrichment in
156 PM_{2.5} relative to potential sources was mainly derived from the isotopic effect of
157 NH₃↔NH₄⁺ equilibrium (assumed as 33‰) (Heaton et al., 1997; Li et al., 2012). At
158 the monitoring site of Beijing, NH₃ could not neutralize abundant SO₂ and NO₂, with
159 an efficient conversion to ammonium salts, little opportunity to volatilize thus no
160 substantial isotopic effect from NH₃↔NH₄⁺ equilibrium (Garten et al., 1992;
161 Yeatman et al., 2001; Kawashima et al., 2011). Therefore, δ¹⁵N values of PM_{2.5} in
162 Beijing are expected to fall in the δ¹⁵N range of verified N sources (Huang et al., 2014;
163 Zhang et al., 2013; Zhang et al., 2015). At the background site, much lower acid gases
164 (especially SO₂) relative to ambient NH₃ could not allow an efficient and quick
165 conversion of NH₃ to ammonium salts. As a result, substantial ¹⁵N enrichment
166 associated NH₃↔NH₄⁺ equilibrium occurred for NH₄⁺ in PM_{2.5} and δ¹⁵N values of
167 PM_{2.5} are expected to be significantly higher than potential sources.

168

169 2 Materials and Methods

170 2.1 Study sites

171 The Beijing site (40°04' N, 116°42' E) was settled in the courtyard of Chinese
172 Research Academy of Environmental Sciences (CRAES), at Lishuiqiao South of
173 Beiyuan Road (surrounded by residential areas, without direct industrial emission
174 sources nearby). As located on the northern edge of the North China Plain, the four



175 seasons of Beijing are characterized by variable meteorological conditions: spring by
176 high-speed winds and low rainfall, summer by high temperature and frequent rain
177 usually accounting for 75% of annual rainfall, autumn by sunny days and northwest
178 winds, and winter by cold and dry air. Due to the urbanization and rapid economic
179 development, there's a huge increase in energy consumption and vehicle quantities,
180 resulted in deterioration of air quality. Air quality monitoring reports of 74 key
181 cities/regions revealed that nearly 70% of urban areas in China could not meet the
182 Ambient Air Quality Standards (GB3095-2012)
183 (http://www.cnemc.cn/publish/106/news/news_34605.html). As the capital of China,
184 a developed megacity in Beijing-Tianjin-Hebei city cluster, Beijing is the foci, not
185 only because of its dense population (more than 20 million inhabitants distributed
186 over 16800km²), but also the ubiquitous air pollution that Beijing has been facing for
187 years. Previous studies showed that atmospheric PM_{2.5} in Beijing were characterized
188 by multiple components and sources, both inorganic to organic constituents, from
189 anthropogenic to natural origins, from primary to secondary components (Duan et al.,
190 2006; Sun et al., 2006; Song et al., 2007). Studies have also proved that secondary
191 inorganic ions (such as SO₄²⁻, NH₄⁺ and NO₃⁻) were the dominant contributors in
192 PM_{2.5} of Beijing (Han et al., 2008; Zhang et al., 2013). During the sampling period of
193 urban site (January 2013), Beijing suffered from the worst PM_{2.5} pollutions in history
194 (<http://cleanairinitiative.org/portal/node/11599>), registering the highest PM_{2.5} hourly
195 concentration of 886 µg/m³ ([http://www.nasa.gov/multimedia/imagegallery/image
196 feature2425.html](http://www.nasa.gov/multimedia/imagegallery/imagefeature2425.html)).

197 The background site (37°36' N, 101°15' E) of this study was located on the
198 Daban Mountain in Menyuan county, northeastern of Qinghai province, which is one
199 of 14 National Background Stations established by the Chinese Ministry of



200 Environmental Protection in 2012. It has a typical Plateau continental climate, with an
201 altitude of 3295m above sea level, a little bit lower than the average of the Tibetan
202 Plateau (about 4000m). The mean annual temperature is -1 – -2 °C and the
203 precipitation is 426 – 860 mm. The mean hourly temperature was 6.5 °C (3 – 11 °C)
204 during the studying period (September 6th – October 15th, 2013). The sampling period
205 belongs to the harvest time after intensive fertilization and pronounced biomass
206 burning. The sampling site is relatively pristine with most areas covered by typical
207 Tibetan Plateau plants. The distance from this site to Xining, the capital City of
208 Qinghai province, is approximately 160 km. There is no locally fossil emission except
209 a national road G227 with few traffic vehicles. Agricultural activity is not intensive
210 locally, except in low-altitude areas far away from the Daban Mountain in Menyuan.
211 Indeed, Menyuan station is an ideal site for monitoring background aerosol and
212 detecting influences of N emissions from human activities (especially biomass
213 burning) on regional atmospheric N chemistry.

214 **2.2 Sample collection and chemical analyses**

215 Sampling was conducted in the autumn of background and in the winter of Beijing,
216 aiming at obtaining typical $\delta^{15}\text{N}$ signals, for testing our hypothesis and partitioning
217 method stated in introduction. Each $\text{PM}_{2.5}$ sample was collected by a pre-baked quartz
218 filter (diameter = 47 mm, sampling area $\approx 13.2 \text{ cm}^2$) using an aerosol sampler (Leckel,
219 MVS6, Germany) equipped with a size-segregating impactor. The operating flow rate
220 was 38.3 L/min. Analyzing N and $\delta^{15}\text{N}$ of $\text{PM}_{2.5}$ at background sites require filter
221 sampling with the duration ranging from days to weeks. The sampling time of
222 individual samples were 47 – 71 hours for samples at the Menyuan site ($n = 14$) and
223 23 hours for CRAES site ($n = 14$), respectively. Filter blanks were assessed in the



224 same manner as the sampling procedure. The PM_{2.5} mass on each filter was
225 gravimetrically measured by the automatic weighting system (AWS-1, COMDE
226 DERENDA, Germany, approved by European Standard) with controlled temperature
227 (20 °C ± 1 °C) and humidity (50 ± 5%) after equilibrated for at least 24 hours, the
228 equipped electro-balance in AWS-1 was WZA26-CW (Sartorius, Germany) with a
229 sensitivity of 0.001 mg. All filter samples collected were stored at -20 °C prior to
230 further analysis. Total N (TN) of PM_{2.5} was measured using three punches (with an
231 area of 0.53 cm² for each punch) of the filter in a vario MACRO cube (Elementar
232 Analysensysteme GmbH, Germany) with an analytical precision of 0.02%. Based on
233 N contents, the δ¹⁵N value of about 50 µg N in each PM_{2.5} sample was determined by
234 a Thermo MAT 253 isotope ratio mass spectrometer (Thermo Scientific, Bremen,
235 Germany) connected with an elemental analyzer (Flash EA 2000). IAEA-N-1
236 (Ammonium Sulfate; δ¹⁵N = 0.4‰), USGS25 (Ammonium Sulfate, δ¹⁵N = -30.4‰),
237 IAEA-NO-3 (Potassium Nitrate; δ¹⁵N = +4.7‰) were measured as standards for the
238 calibration of δ¹⁵N values. The average standard deviations for replicate analyses of
239 an individual sample was ±0.1‰. TN concentrations, δ¹⁵N values are reported as the
240 average of three replicated measurements per sample. The natural abundance of ¹⁵N
241 (δ¹⁵N) in PM_{2.5} was expressed in parts per thousand (per mille) by multiplying them
242 by 1000:

$$243 \delta^{15}\text{N} = (R_{\text{sample}} / R_{\text{standard}}) - 1,$$

244 where $R = {}^{15}\text{N}/{}^{14}\text{N}$ for samples and standard (atmospheric N₂).

245 The concentrations of NO₃⁻, NH₄⁺, SO₄²⁻ in PM_{2.5} were measured during the
246 sampling period at both sites by an ambient ion monitor (AIM-IC system: Model
247 URG 9000B, URG Corporation, USA). The real-time instruments installed at both
248 stations have good performance for above water-soluble ions, with a detection limit as



249 0.05 $\mu\text{g}/\text{m}^3$. It draws air in through a $\text{PM}_{2.5}$ sharp-cut cyclone at a volumetric-flow
250 controlled rate of 3 L/min to remove the larger particles from the air stream. Gases
251 (e.g., SO_2 , NH_3 , and HNO_3) are stripped from the air stream by passing through a
252 liquid parallel plate denuder with continuously replenished solvent flowing across the
253 surface. Then the $\text{PM}_{2.5}$ air stream are constrained into a supersaturated steam
254 condensation coil and cyclone assembly and grown hygroscopically for collection.
255 Enlarged particles are dissolved in water solutions for anion chromatographic analysis
256 every hour following 60 minutes of ambient sampling. Concentrations of NO_2 were
257 measured using a $\text{NO}-\text{NO}_2-\text{NO}_x$ chemiluminescence analyzer (Model 42i,
258 Thermo-Fisher Scientific). The instruments were operated and maintained properly to
259 ensure data integrity. Scheduled quality control procedures included daily zero and
260 span checks, weekly precision checks and data validations.

261

262 3 Results

263 At the Beijing site (CRAES), the mean $\text{PM}_{2.5}$ level reached $264.3 \pm 118.0 \mu\text{g}/\text{m}^3$ (43.0
264 $- 433.6 \mu\text{g}/\text{m}^3$) over the studying haze episode in January 2013, which was 20 times
265 higher than that at the background site (Tables 1 and S1). Volumetric concentrations
266 of elements and ions in $\text{PM}_{2.5}$ differed distinctly between the two studying sites, thus
267 they were presented as mass concentrations of $\text{PM}_{2.5}$ for comparison. The mass
268 concentrations and $\delta^{15}\text{N}$ values of TN in $\text{PM}_{2.5}$ at Beijing site averaged $16.7 \pm 4.6\%$
269 ($8.2 - 29.3\%$) and $+2.8 \pm 6.4\%$ ($-4.1 - +13.5\%$), respectively (Tables 1 and S1; Fig.
270 1). Concentrations of NH_4^+-N , NO_3^--N and $\text{SO}_4^{2--}\text{S}$ in $\text{PM}_{2.5}$ mass averaged $7.4 \pm$
271 3.4% , $5.0 \pm 3.0\%$, $5.5 \pm 2.4\%$, respectively at Beijing site, showing mean molecular
272 ratios of NH_4^+ to NO_3^- , NH_4^+ to SO_4^{2-} , NH_4^+ to $(\text{NO}_3^- + \text{SO}_4^{2-})$, NH_4^+ to $(\text{NO}_3^- +$



273 $1/2*\text{SO}_4^{2-}$) as 2.5, 3.5, 1.1, 1.4, respectively (Table 1). Ambient concentrations of NO_2
274 averaged $89.2 \pm 21.2 \mu\text{g}/\text{m}^3$ at Beijing (Table 1). Mean concentrations of ambient
275 NH_3 (during April of 2013) and SO_2 (during January of 2013) were reported as 14.1
276 and $22.9 \mu\text{g}/\text{m}^3$, respectively (He et al., 2014; Wei et al., 2015). Using these data,
277 mean molecular ratios of NH_3 to NO_2 , NH_3 to SO_2 , NH_3 to $(\text{NO}_2 + \text{SO}_2)$, NH_3 to $(\text{NO}_2$
278 $+ 1/2*\text{SO}_2)$ were 0.4, 2.3, 0.4, 0.4, respectively (Table 1).

279 At the background site (Menyuan, Qinghai province), the filter-based
280 concentrations of atmospheric $\text{PM}_{2.5}$ averaged $13.0 \pm 3.2 \mu\text{g}/\text{m}^3$ ($7.0 - 17.8 \mu\text{g}/\text{m}^3$)
281 during the studying period (September 6th – October 15th, 2013) (Tables 1 and S1),
282 which was almost the same as that ($13.0 \pm 4.8 \mu\text{g}/\text{m}^3$; $4.6 - 22.7 \mu\text{g}/\text{m}^3$) based on an
283 ambient monitor (AIM-IC system: Model URG 9000B, URG Corporation, USA). The
284 mass concentrations and $\delta^{15}\text{N}$ values of TN in $\text{PM}_{2.5}$ at the background site averaged
285 $8.6 \pm 5.6\%$ and $+18.5 \pm 5.8\%$ ($+8.0 - +27.9\%$) (Tables 1 and S1; Fig. 1).
286 Concentrations of $\text{NH}_4^+\text{-N}$, $\text{NO}_3^-\text{-N}$ and $\text{SO}_4^{2-}\text{-S}$ in the mass of $\text{PM}_{2.5}$ at Menyuan
287 averaged $5.9 \pm 1.8\%$, $1.9 \pm 0.4\%$, $0.2 \pm 0.0\%$, respectively (Table 1), showing mean
288 molecular ratios of $\text{NH}_4^+/\text{NO}_3^-$, $\text{NH}_4^+/\text{SO}_4^{2-}$, $\text{NH}_4^+/(\text{NO}_3^- + \text{SO}_4^{2-})$, $\text{NH}_4^+/(\text{NO}_3^- +$
289 $1/2*\text{SO}_4^{2-})$ as 3.3, 56.3, 3.1, 3.2, respectively (Table 1). Ambient concentrations of
290 NO_2 averaged $4.3 \pm 1.3 \mu\text{g}/\text{m}^3$ at the background site (Table 1). Ambient NH_3 and
291 SO_2 concentrations were not available at the Menyuan site ($37^\circ 36' \text{N}$, $101^\circ 15' \text{E}$;
292 3295m), but the other background site in the same province (Waliguan, Qinghai;
293 $36^\circ 30' \text{N}$, $100^\circ 10' \text{E}$, 3816m ; a global baseline station) showed mean atmospheric
294 NH_3 and SO_2 concentrations as $4.8 \mu\text{g}/\text{m}^3$ and $0.31 \mu\text{g}/\text{m}^3$ (Carmichael et al., 2003),
295 showing mean molecular ratios of NH_3 to NO_2 , NH_3 to SO_2 , NH_3 to $(\text{NO}_2 + \text{SO}_2)$,
296 NH_3 to $(\text{NO}_2 + 1/2*\text{SO}_2)$ as 3.0, 60.2, 2.9, 2.9, respectively (Table 1).



297

298 **4 Discussions**

299 **4.1 Major sources and isotopic effect**

300 Natural ^{15}N isotope method can examine contributions of multiple N sources to a
301 given mixture pool, but a reasonable judgment of dominant sources is critical. At
302 Beijing site, six dominant N sources were assigned for TN in $\text{PM}_{2.5}$ samples collected
303 during the severe haze episode of January 2013:

304 S0: TN in soil dust,

305 S1: NO_2 from coal combustion,

306 S2: NH_3 from coal combustion,

307 S3: NO_2 from vehicle exhausts,

308 S4: NH_3 from vehicle exhausts,

309 S5: NH_3 from domestic wastes/sewage.

310 These putative origins have also been recognized to be responsible for PM pollution
311 during the severe haze episode of January 2013 (Zhang et al., 2013, 2015; Huang et
312 al., 2014). The mean $\delta^{15}\text{N}$ of soils (+6.0‰) was assumed as that of soil dust (Wang et
313 al., 2014), because the sampling time and sites of soil fit the air mass backward
314 trajectories of our studying sites (Fig. 2). So far, $\delta^{15}\text{N}$ values of NO_2 and NH_3
315 emissions are unavailable in many countries, but they were distinctive among most
316 typical sources and N species (Table S2, Fig. 1). Representative $\delta^{15}\text{N}$ values reported
317 for NO_2 and NH_3 emissions were adopted in our partitioning method (Table S2). But
318 we did not consider precursor $\delta^{15}\text{N}$ data which was influenced by post-emission
319 processes (e.g., roadside and tunnel because they can mix with other sources), and
320 measured through controlled tests or simulation. For examples, we did not use the
321 $\delta^{15}\text{N}$ data of NH_3 near highway (-5.0 – +0.4‰ in Smirnov et al., 2012), NO_2 near



322 highway (+2 – +10‰ in Moore et al., 1977, Ammann et al., 1999, Pearson et al., 2000;
323 -13.3 – +0.4‰ in Smirnoff et al., 2012), NO₂ in tunnels (+15.0 ± 1.6‰ for NO₂; +5.7
324 ± 2.8‰ for HNO₃ in Felix et al., 2014), NO₂ from vehicle engine (-13.0 – +3.7‰ in
325 Moore, 1977; Heaton, 1990; Freyer, 1978a,b, 1991), NO₂ from controlled
326 experiments of diesel combustion (+3.9 – +5.4‰ in Widory, 2007) and coal
327 combustion (-5.3‰ in Widory, 2007). Besides, the agricultural and biogenic N
328 emissions (mainly biomass burning, fertilizer application, animal wastes) were not
329 considered as sources of the urban PM_{2.5} samples three reasons. First, these emissions
330 (mainly NH₃ if any) are less dispersible and long-distance transported. Second, the
331 CRAES site is located in the center of Beijing city cluster. Third, there was a severe
332 haze pollution event during our sampling time (January, 2013) (Huang et al., 2014).
333 We assumed a negligible contribution from NH₃ emission from seawater ($\delta^{15}\text{N} = -8 -$
334 -5% in Jickells et al., 2003) and lightning NO₂ ($\delta^{15}\text{N} = -0.5 - +1.4\%$ (Hoering et al.,
335 1957) because aerosols in inland urban environments derive almost all N from
336 land-based sources thus have a greater anthropogenic imprint. The lightning NO₂ can
337 be quickly scavenged by precipitation during the rain events, with little diffusion and
338 contribution to N in near-surface particulates.

339 At the Menyuan background site, potential sources of N in PM_{2.5} include:

- 340 S0: TN in soil dust,
- 341 S6: NO₂ from biomass burning,
- 342 S7: NH₃ from biomass burning,
- 343 S8: NO₂ from animal wastes,
- 344 S9: NH₃ from animal wastes,
- 345 S10: NO₂ from soil N cycle,
- 346 S11: NH₃ from fertilizer application.



347 We inferred a significant contribution from agricultural N (especially NH_3) emissions
348 to the background $\text{PM}_{2.5}$ due to two reasons. First, the N of background $\text{PM}_{2.5}$ was
349 dominated by NH_4^+ -N (Table 1). Second, $\delta^{15}\text{N}$ values of $\text{PM}_{2.5}$ should assemble or
350 lower than that of soil N and NO_2 if no influence from agricultural NH_3 sources.
351 However, the observed $\delta^{15}\text{N}$ values of $\text{PM}_{2.5}$ at the background site fall in a range
352 much higher than isotopic values of potential sources and most anthropogenic sources
353 (Table S2, Fig. 1). Due to the dominance of NH_4 -N in $\text{PM}_{2.5}$ and NH_3 in ambient
354 atmosphere (Table 1), the ^{15}N enrichment in $\text{PM}_{2.5}$ at the background site was mainly
355 attributed to a significant isotope fractionation during the equilibrium between NH_3
356 and NH_4^+ (33%; Heaton et al., 1997).

357 Here we provide possible reasons and mechanisms to explain why $\delta^{15}\text{N}$ values of
358 $\text{PM}_{2.5}$ assembled those of recognized sources at Beijing site, but were higher than
359 potential sources at the background site of Qinghai (Fig. 1). At the CRAES site of
360 Beijing, molecular ratios of ambient NH_3 to $(\text{NO}_2 + \text{SO}_2)$ or to $(\text{NO}_2 + 1/2*\text{SO}_2)$ (<1;
361 Table 1) reflected a more thorough neutralization of NH_3 by acidic gases, producing
362 relatively more stable ammonium salts of NH_4NO_3 , NH_4HSO_4 and $(\text{NH}_4)_2\text{SO}_4$.
363 Molecular ratios of NH_4^+ to $(\text{NO}_3^- + \text{SO}_4^{2-})$ or to $(\text{NO}_3^- + 1/2*\text{SO}_4^{2-})$ in $\text{PM}_{2.5}$ (close to
364 1:1; Table 1) also verified that NH_3 reacts mainly with SO_2 and NO_2 . Consequently,
365 the equilibrium between NH_3 and NH_4^+ was weak or did not cause significant isotope
366 fractionation for NH_4^+ of $\text{PM}_{2.5}$ and $\delta^{15}\text{N}$ values of $\text{PM}_{2.5}$ distributed within those of
367 recognized sources at Beijing site (Fig. 1).

368 Differently, molecular ratios of atmospheric NH_3 to $(\text{NO}_2 + \text{SO}_2)$ or to $(\text{NO}_2 +$
369 $1/2*\text{SO}_2)$ were high as 2.9 at the background site (Menyuan, Qinghai) (Table 1),
370 illustrating an incomplete neutralization of NH_3 by NO_2 and SO_2 . Molecular ratios of
371 NH_4^+ to $(\text{NO}_3^- + \text{SO}_4^{2-})$ or to $(\text{NO}_3^- + 1/2*\text{SO}_4^{2-})$ in $\text{PM}_{2.5}$ (close to 3; Table 1) also



372 suggested that part of ammonium existed as relative unstable salts (e.g., NH_4Cl). Most
 373 likely, the reversible reaction and a strong equilibrium between NH_3 and NH_4^+
 374 occurred, the diffusion of NH_3 back to the atmosphere caused significant ^{15}N
 375 enrichment in NH_4^+ of $\text{PM}_{2.5}$. As a result, $\delta^{15}\text{N}$ values of $\text{PM}_{2.5}$ were higher than
 376 potential sources at the background site of Qinghai (Fig. 1). The regulation of acidic
 377 gases-to- NH_3 stoichiometry on the reaction and isotopic effect between NH_3 and
 378 NH_4^+ was supported by a positive correlation between $\delta^{15}\text{N}$ values and $\text{NH}_4^+ / (\text{NO}_3^- +$
 379 $1/2 * \text{SO}_4^{2-})$ ratios in $\text{PM}_{2.5}$ (Fig. 3). Therefore, $\delta^{15}\text{N}$ values of $\text{PM}_{2.5}$ in Beijing site
 380 reflected a mixing of major sources with no appreciable isotopic effects, thus support
 381 direct isotope estimation by IsoSource. However, a net isotope effect of $\text{NH}_3(g) \leftrightarrow$
 382 $\text{NH}_4^+(p)$ equilibrium ($\epsilon_{\text{eq}} = 33\text{‰}$ in Heaton et al., 1997) should be added to NH_3
 383 sources before inputting into IsoSource for calculations (details down in Section 4.2).

384 4.2 Fractional contributions of major sources to N in $\text{PM}_{2.5}$

385 The proportional contributions (f , %) of major sources to N in $\text{PM}_{2.5}$ are calculated
 386 using the IsoSource model (Phillips et al., 2003). For urban $\text{PM}_{2.5}$,

$$387 \delta^{15}\text{N}_{\text{PM}_{2.5}(\text{Beijing})} = \delta^{15}\text{N}_{\text{S0}} \times f_{\text{S0}} + \delta^{15}\text{N}_{\text{S1}} \times f_{\text{S1}} + \delta^{15}\text{N}_{\text{S2}} \times f_{\text{S2}} + \delta^{15}\text{N}_{\text{S3}} \times f_{\text{S3}} + \delta^{15}\text{N}_{\text{S4}} \times f_{\text{S4}}$$

$$388 + \delta^{15}\text{N}_{\text{S5}} \times f_{\text{S5}} \text{ (Equation 1).}$$

389 For background $\text{PM}_{2.5}$,

$$390 \delta^{15}\text{N}_{\text{PM}_{2.5}(\text{Background})} = \delta^{15}\text{N}_{\text{S0}} \times f_{\text{S0}} + \delta^{15}\text{N}_{\text{S6}} \times f_{\text{S6}} + (\delta^{15}\text{N}_{\text{S7}} + \epsilon_{\text{eq}}) \times f_{\text{S7}} + \delta^{15}\text{N}_{\text{S8}} \times f_{\text{S8}} +$$

$$391 (\delta^{15}\text{N}_{\text{S9}} + \epsilon_{\text{eq}}) \times f_{\text{S9}} + \delta^{15}\text{N}_{\text{S10}} \times f_{\text{S10}} + (\delta^{15}\text{N}_{\text{S11}} + \epsilon_{\text{eq}}) \times f_{\text{S11}} \text{ (Equation 2), where } \epsilon_{\text{eq}} \text{ is}$$

$$392 33\text{‰} \text{ (Heaton et al., 1997).}$$

393 The IsoSource model iteratively generates source isotopic mixtures of which the
 394 proportions (f) sum to 1 (in Equation 1: $f_{\text{S0}} + f_{\text{S1}} + f_{\text{S2}} + f_{\text{S3}} + f_{\text{S4}} + f_{\text{S5}} = 1$ for urban
 395 $\text{PM}_{2.5}$; In Equation 2: $f_{\text{S0}} + f_{\text{S6}} + f_{\text{S7}} + f_{\text{S8}} + f_{\text{S9}} + f_{\text{S10}} + f_{\text{S11}} = 1$ for background $\text{PM}_{2.5}$). It



396 compares each calculation against a known mixture ($\delta^{15}\text{N}$ of $\text{PM}_{2.5}$ samples; Table S1)
397 and retains only those mixtures that satisfy the known $\delta^{15}\text{N}$ value within some mass
398 balance tolerance. This model provides a systematic mode of constraining the
399 attribution of N sources in an underdetermined system. In our case, the calculated
400 mixtures reflected combinations of precursor $\delta^{15}\text{N}$ values of dominant sources (Table
401 S2) and N in collected $\text{PM}_{2.5}$ samples. We applied a mass balance tolerance of 0.02.
402 The mean values of output percentages from the model are adopted for the fractional
403 contribution of each source to TN in each $\text{PM}_{2.5}$ replicate sample. Then the range and
404 mean values of all replicate samples are presented for each source at Beijing or
405 background site (Fig. 4).

406 There was no difference in the fractional contributions of N from soil dusts
407 between Beijing ($14 \pm 5\%$) and background ($12 \pm 3\%$) $\text{PM}_{2.5}$ samples (Fig. 4). This
408 reflected a fundamental nucleus of soil dust for the formation of $\text{PM}_{2.5}$ (He et al.,
409 2014). During the haze episode of January 2013 in Beijing, low fractions of the
410 primary aerosol constituents (e.g., mineral dusts, black carbon) and high fractions of
411 N from secondary processes have been demonstrated (Huang et al., 2014). Our
412 estimation showed that NO_2 contributed more N to $\text{PM}_{2.5}$ at Beijing site ($f_{\text{NO}_2(\text{Beijing})} =$
413 $41 \pm 19\%$) than that at the background site ($f_{\text{NO}_2(\text{Menyuan})} = 30 \pm 8\%$) (Table 2). The
414 mean ratio of f_{NH_3} to f_{NO_2} in N of $\text{PM}_{2.5}$ was generally higher at the background site
415 (2.3 ± 1.1) than that at Beijing site (1.5 ± 1.1) (Table 2), which generally followed the
416 pattern of $\text{NH}_4^+/\text{NO}_3^-$ ratios in $\text{PM}_{2.5}$ (Table 1). In fact, the contributing ratios of
417 precursors can neither be exactly verified by the ratios of $\text{NH}_4^+/\text{NO}_3^-$ in $\text{PM}_{2.5}$, nor by
418 the ratios of gaseous NH_3/NO_2 in the atmosphere. Firstly, NO_2 and NH_3 precursors
419 can substantially react with organic compounds to form organic N compounds. The
420 severe haze pollution event in January 2013 of Beijing was driven by both secondary



421 inorganic and organic aerosols (Huang et al., 2014). Secondly, the gas-to-particle
422 reaction rates differ between NO_2 and NH_3 , the distributions of N ions or compounds
423 differ among particles with different aerodynamic diameters, between NO_2 and NH_3 .
424 Thirdly, the abundance of SO_2 can make the ratios of NO_3^- to NH_4^+ difficult to follow
425 those of ambient NO_2 to NH_3 . The concentrations of NO_3^- and NH_4^+ in particles can
426 be more sensitive to changes in SO_2 than in its own precursor emissions (Lei and
427 Wuebbles, 2013; He et al., 2014).

428 On average, 86% of N in $\text{PM}_{2.5}$ at Beijing site was anthropogenic, in which 71%
429 was derived from fossil fuel combustion and NO_2 from coal burning was the biggest
430 contributor (26%) (Table 2). Regarding to fossil-derived N sources, coal combustion
431 contributed more N (41%) than traffic emissions (30%), NO_2 contributed more N
432 (41%) than NH_3 (30%) (Table 2). Coal combustion and traffic emissions had the same
433 contribution (15% to TN) in fossil-derived NH_3 , NH_3 and NO_2 had the same
434 contribution (15% to TN) in vehicle-derived N (Table 2). These results demonstrated
435 that fossil fuel-based NH_3 emissions substantially contributed to $\text{PM}_{2.5}$ N pollution in
436 densely populated urban areas. In particular, vehicles equipped with three-way
437 catalytic converters, electrical generating units and units with selective catalytic
438 reduction or selective non-catalytic NO_2 reduction technologies should be significant
439 ‘fuel NH_3 ’ sources (Cape et al., 2004; Kirchner et al., 2005). Our results
440 unambiguously illustrate that regulatory controls of NO_2 emissions from coal burning
441 (nearby industrial facilities) and NH_3 from urban transportation is important to avert
442 the risk of severe haze episodes in Beijing. It should be noted that 29% of N in urban
443 $\text{PM}_{2.5}$ was from non-fossil N sources (domestic wastes/sewage and soil dust) (Table 2).
444 Before this, non-fossil contribution to $\text{PM}_{2.5}$ mass was shown as ~15% (only primary
445 and secondary organic aerosols were considered) in Beijing during the severe haze



446 event of January 2013 (Huang et al., 2014). However, higher non-fossil contribution
447 (35% of $PM_{2.5}$ mass) was observed at five cities of the Yangtze River Delta, China
448 (Cheng et al., 2011). At the background site, N in $PM_{2.5}$ was not dominated by natural
449 and biogenic N emissions, but by agricultural N sources ($82 \pm 7\%$; Table 2). In total,
450 NH_3 from animal wastes/excreta and fertilizer accounted for only 17%, but biomass
451 burning had the highest contribution (58%) in N of $PM_{2.5}$ at the background site
452 (Table 2). Moreover, biomass burning contributed more N as NH_3 (44%) than as NO_2
453 (14%) to N of $PM_{2.5}$ at the background site (Table 2). Higher production of NH_3 than
454 NO_2 from biomass burning have been documented previously (Hegg et al., 1988;
455 Crutzen and Andreae, 1990). A burning experiment by Lobert et al (1990) also
456 showed that the emission ratio of NH_3 (3.8%) was higher than that of SO_2 (0.3%)
457 during biomass burning. Andreae and Merlet (2001) further clarified that the emission
458 factors of NH_3 were 2 – 5 times higher than that of SO_2 from various types of biomass
459 burning. Our results revealed an important contribution of biomass-burning NH_3 to
460 the formation of secondary $PM_{2.5}$ at rural and background sites.

461

462 5 Conclusions

463 This paper provides a natural isotope method to quantify contributions of major
464 source precursors to N in atmospheric particulates based on TN of $PM_{2.5}$ at Beijing
465 and a background site. Significant ^{15}N enrichment in $PM_{2.5}$ relative to potential
466 sources was observed at the background site, not at Beijing site. Combined with
467 evidences from the chemistry of local $PM_{2.5}$ and precursors, a significant isotopic
468 effect of $NH_3 \leftrightarrow NH_4^+$ equilibrium was recognized under the condition of lower acid
469 gases (especially SO_2) relative to ambient NH_3 , which should be considered into the
470 fractional estimation of NH_3 in TN of $PM_{2.5}$. Based on calculating results of IsoSource,



471 PM_{2.5} of Beijing derived N mainly came from coal combustion (41%), vehicle
472 exhausts (30%) and domestic wastes/sewage (14%), while background PM_{2.5} derived
473 N mainly came from biomass burning (58%), animal wastes (15%) and fertilizer
474 application (9%). Regulatory controls of NO₂ emissions from coal burning and NH₃
475 from urban transportation is still an important and effective step to reduce the risk of
476 the formation of severe haze episodes in Chinese cities. However, emissions of N
477 from biomass burning in broad rural areas should be stressed to meet a rigorous
478 reduction of reactive N emissions in China.

479

480 **Acknowledgements.** This work was supported by the State Environmental Protection
481 Commonweal Trade Scientific Research, Ministry of Environmental Protection of
482 China (No. 2013467010) and the National Natural Science Foundation of China (Nos.
483 41273026, 41522301). Xue-Yan Liu was also supported by the 11st Recruitment
484 Program of Global Experts (the Thousand Talents Plan) for Young Professionals
485 granted by the central budget of China, and Youth Innovation Promotion Association
486 of Chinese Academy of Sciences (No. 2015327). All the financial support from fund
487 and research support from the staff of CRAES are gratefully acknowledged.
488

489 **References**

- 490 Ammann, M., Siegwolf, R., Pichlmayer, F., Suter, M., Saurer, M., Brunold, C.: Estimating the
491 uptake of traffic-derived NO₂ from ¹⁵N abundance in Norway spruce needles, *Oecologia*, 118,
492 124-131, 1999.
- 493 Andreae M. O. and Metlet P.: Emission of trace gases and aerosols from biomass burning. *Glob*
494 *Biogeochem Cy*, 15 (4), 955-966, doi: 10.1029/2000GB001382. 2001.
- 495 Cao, F. & Zhang, Y. L.: Tightening nonfossil emissions control: A potential opportunity for PM_{2.5}
496 mitigation in China, *Proc Natl Acad Sci USA*, 112 (12) E1402, doi:
497 10.1073/pnas.1423532112, 2015.
- 498 Cape, J. N., Tang, Y. S., van Dijk, N., Love, L., Sutton, M. A., Palmer, S. C. F.: Concentrations of
499 ammonia and nitrogen dioxide at roadside verges, and their contribution to nitrogen
500 deposition, *Environ. Pollut.*, 132, 469-478, doi: 10.1016/j.envpol.2004.05.009, 2004.
- 501 Cheng, Z., Wang, S., Fu, X., Watson, J. G., Jiang, J., Fu, Q., Chen, C., Xu, B., Yu, J., Chow, J. C.,



- 502 Hao, J. M.: Impact of biomass burning on haze pollution in the Yangtze River delta, China: a
503 case study in summer 2011, Atmos. Chem. Phys., 14(9), 4573-4585, doi:
504 10.5194/acp-14-4573-2014, 2011.
- 505 China National Environmental Monitoring Centre. Air Quality Report in 74 Chinese Cities in
506 March and the First Quarter 2013
507 (http://www.cnemc.cn/publish/106/news/news_34605.html).
- 508 Clean-Air-Asia. Beijing's Air Pollution Episode (January 2013), available at:
509 <http://cleanairinitiative.org/portal/node/11599>.
- 510 Crutzen, P. J. & Andreae, M. O.: Biomass burning in the tropics: Impact on atmospheric
511 chemistry and biogeochemical cycles, Science, 250, 1669-1678, 1990.
- 512 Divers, M. T., Elliott, E. M., Bain, D. J.: Quantification of nitrate sources to an urban stream using
513 dual nitrate isotopes, Environ. Sci. Technol., 48(18), 10,580-510,587, doi: 10.1021/es404880j,
514 2014.
- 515 Duan, F. K., He, K. B., Ma, Y. L., Yang, F. M., Yu, X. C., Cadle, S. H., Chan, T., Mulawa, P. A.:
516 Concentration and chemical characteristics of PM_{2.5} in Beijing, China: 2001–2002, Sci. Total
517 Environ., 355, 264-275, doi: 10.1016/j.scitotenv.2005.03.001, 2006.
- 518 Elliott, E. M., Kendall, C., Boyer, E. W., Burns, D. A., Lear, G., Golden, H. E., Harlin, K.,
519 Bytnerowicz, A., Butler, T. J., Glatz, R.: Dual nitrate isotopes in actively and passively
520 collected dry deposition: Utility for partitioning NO_x sources contributing to landscape
521 nitrogen deposition, J. Geophys. Res. Biogeosci, 114, G04020, doi: Artn
522 G0402010.1029/2008jg000889, 2009.
- 523 Elliott, E. M., Kendall, C., Wankel, S. D., Burns, D. A., Boyer, E. W., Harlin, K., Bain, D. J.,
524 Butler, T. J.: Nitrogen isotopes as indicators of NO_x source contributions to atmospheric
525 nitrate deposition across the Midwestern and Northeastern United States, Environ. Sci.
526 Technol., 41, 7661-7667, doi: 10.1021/es070898t, 2007.
- 527 Felix, J. D. and Elliott, E. M.: The isotopic composition of passively collected nitrogen dioxide
528 emissions: Vehicle, soil and livestock source signatures, Atmos. Environ., 92, 359-366, doi:
529 10.1016/j.atmosenv.2014.04.005, 2014.
- 530 Felix, J. D., Elliott, E. M., Gish, T., Magrihang, R., Clougherty, J., Cambal, L.: Examining the



- 531 transport of ammonia emissions across landscapes using nitrogen isotope ratios, Atmos.
532 Environ., 95, 563-570, doi:10.1016/j.atmosenv.2014.06.061,2014.
- 533 Felix, J. D., Elliott, E. M., Gish, T., McConnell, L., Shaw, S.: Characterizing the isotopic
534 composition of atmospheric ammonia emission sources using passive samplers and a
535 combined oxidation-bacterial denitrifier isotope ratio mass spectrometer method, Rapid.
536 Commun. Mass Sp., 27(20), 2239-2246, doi: 10.1002/rcm.6679, 2013.
- 537 Felix, J. D., Elliott, E. M., Shaw, S. L.: The isotopic composition of coal-fired power plant NO_x:
538 The influence of emission controls and implications for global emission inventories, Environ.
539 Sci. Technol., 46 (6), 3528-3535, doi: 10.1021/es203355v, 2012.
- 540 Feng, J., Li, M., Zhang, P., Gong, S., Zhong, M., Wu, M., Zheng, M., Chen, C., Wang, H., Lou, S.:
541 Investigation of the sources and seasonal variations of secondary organic aerosols in PM_{2.5} in
542 Shanghai with organic tracers, Atmos. Environ., 79, 614-622, doi:
543 10.1016/j.atmosenv.2013.07.022, 2013.
- 544 Frank, D. A., Evans, R. D., Tracy, B. F.: The role of ammonia volatilization in controlling the
545 natural ¹⁵N abundance of a grazed grassland, Biogeochemistry, 68, 169-178, doi:
546 10.1023/B:Biog.0000025736.19381.91, 2004.
- 547 Freyer, H.: Seasonal variation of ¹⁵N/¹⁴N ratios in atmospheric nitrate species, Tellus B, 43,
548 30-44, 1991.
- 549 Fu, X., Guo, H., Wang, X., Ding, X., He, Q., Liu, T., Zhang, Z.: PM_{2.5} acidity at a background site
550 in the Pearl River Delta region in fall-winter of 2007–2012, J. Hazard. Mater., 286, 484-492,
551 doi: 10.1016/j.jhazmat.2015.01.022, 2015.
- 552 Fukuzaki, N. and Hayasaka, H.: Seasonal variations of nitrogen isotopic ratios of ammonium and
553 nitrate in precipitations collected in the Yahiko-Kakuda Mountains Area in Niigata
554 Prefecture, Japan, Water, Air, & Soil Pollut., 203, 391-397, doi: 10.1007/s11270-009-0026-8,
555 2009.
- 556 Garten, J. C. T.: Nitrogen isotope composition of ammonium and nitrate in total precipitation and
557 forest throughfall, Int. J. of Environ. Anal. Chem., 47, 33-45, 1992.
- 558 Ge, XL., Wexler, A. S., Clegg, S. L.: Atmospheric amines Part I. A review, Atmos. Environ., 45,
559 524-546, doi:10.1016/j.atmosenv.2010.10.012. 2011.



- 560 Ge, X.L., Wexler, A. S., Clegg, S. L.: Atmospheric amines Part II. Thermodynamic properties and
561 gas/particle partitioning, *Atmos. Environ.*, 45, 561-577, doi:10.1016/j.atmosenv.2010.10.013.
562 2011.
- 563 Guo, S., Hu, M., Zamora, M. L., Peng, J., Shang, D., Zheng, J., Du, Z., Wu, Z., Shao, M., Zeng, L.,
564 Molina, M. J., Zhang, R.: Elucidating severe urban haze formation in China, *Proc Natl Acad*
565 *Sci USA*, 111(49), 17373-17378, doi: 10.1073/pnas.1419604111, 2014.
- 566 Han, Y. J., Kim, T. S., Kim, H. K.: Ionic constituents and source analysis of PM_{2.5} in three Korean
567 cities, *Atmos. Environ.*, 42, 4735-4746, doi: 10.1016/j.atmosenv.2008.01.047, 2008.
- 568 Heaton, T. H. E., Spiro, B., Roberston, S. M. C.: Potential canopy influences on the isotopic
569 composition of nitrogen and sulphur in atmospheric deposition, *Oecologia*, 109, 600-660,
570 1997.
- 571 Heaton, T. H. E., Wynn, P., Tye, A. M.: Low ¹⁵N/¹⁴N ratios for nitrate in snow in the High Arctic
572 (79 ‰), *Atmos. Environ.*, 38, 5611-5621, doi: 10.1016/j.atmosenv.2004.06.028, 2004.
- 573 Heaton, T. H. E.: ¹⁵N/¹⁴N ratios of NO_x from vehicle engines and coal-fired power stations, *Tellus*,
574 42, 304-307, 1990.
- 575 Heaton, T. H. E.: Isotopic studies of nitrogen pollution in the hydrosphere and atmosphere: a
576 review, *Chem. Geol.*, 59, 87-102, 1986.
- 577 Hegg, D. A., Radke, L. F., Hobbs, P. V.: Ammonium emissions from biomass burning. *Geophys*
578 *Res Lett*, 15 (4), 335-337, 1988.
- 579 Hoering, T.: The isotopic composition of ammonia and the nitrate ion in rain, *Geochim*
580 *Cosmochim Acta.*, 12, 97-102, 1957.
- 581 Huang, R. J., Zhang, Y. L., Bozzetti, C., Ho, K. F., Cao, J. J., Han, Y., Daellenbach, K. R., Slowik,
582 J. G., Platt, S. M., Canonaco, F., Zotter, P., Wolf, R., Pieber, S. M., Brun, E. A., Crippa, M.,
583 Ciarelli, G., Piazzalunga, A., Schwikowski, M., Abbaszade, G., Schnelle-Kreis, J.,
584 Zimmermann, R., An, Z., Szidat, S., Baltensperger, U., El Haddad, I., Prevot, A. S.: High
585 secondary aerosol contribution to particulate pollution during haze events in China, *Nature*,
586 514, 218-222, doi: 10.1038/nature13774, 2014.
- 587 Jia, G. & Chen, F.: Monthly variations in nitrogen isotopes of ammonium and nitrate in wet
588 deposition at Guangzhou, south China, *Atmos. Environ.*, 44, 2309-2315, doi:



- 589 10.1016/j.atmosenv.2010.03.041, 2010.
- 590 Kawashima, H. and Kurahashi, T.: Inorganic ion and nitrogen isotopic compositions of
591 atmospheric aerosols at Yurihonjo, Japan: Implications for nitrogen sources, Atmos. Environ.,
592 45, 6309-6316, doi: 10.1016/j.atmosenv.2011.08.057, 2011.
- 593 Kendall, C., Elliott, E. M., Wankel, S. D.: Tracing anthropogenic inputs of nitrogen to ecosystems
594 In Stable Isotopes in Ecology and Environmental Science., Michener, RM, Lajtha, KE.
595 Blackwell.Oxford, 375-449, 2007.
- 596 Kiga, T., Watanabe, S., Yoshikawa, K., Asano, K., Okitsu, S., Tsunogai, U., Narukawa, K.
597 Evaluation of NO_x formation in pulverized coal firing by use of nitrogen isotope ratios,
598 Presented at ASME 2000 International Joint Power Generation Conference, Miami Beach,
599 FL, July 23-26, 2000, ASME: Miami Beach, FL.
- 600 Kirchner, M., Jakobi, G., Feicht, E., Bernhardt, M., Fischer, A.: Elevated NH₃ and NO₂ air
601 concentrations and nitrogen deposition rates in the vicinity of a highway in Southern Bavaria,
602 Atmos. Environ., 39, 4531-4542, doi: 10.1016/j.atmosenv.2005.03.052, 2005.
- 603 Kundu, S., Kawamura, K., Lee, M.: Seasonal variation of the concentrations of nitrogenous
604 species and their nitrogen isotopic ratios in aerosols at Gosan, Jeju Island: implications for
605 atmospheric processing and source changes of aerosols, J. Geophys. Res., 115, D20305, doi:
606 Artn D2030510.1029/2009jd013323, 2010.
- 607 Laffray, X., Rose, C., Garrec, J.P.: Biomonitoring of traffic-related nitrogen oxides in the
608 Maurienne valley (Savoie, France), using purple moor grass growth parameters and leaf
609 ¹⁵N/¹⁴N ratio, Environ. Pollut., 158, 1652-1660, doi:10.1016/j.envpol.2009.12.005, 2010.
- 610 Lei, H. & Wuebbles, D.: Chemical competition in nitrate and sulfate formations and its effect on
611 air quality, Atmos. Environ., 80, 472-477, doi: 10.1016/j.atmosenv.2013.08.036, 2013.
- 612 Li, D. J., Wang, X. M.: Nitrogen isotopic signature of soil-released nitric oxide (NO) after
613 fertilizer application, Atmos. Environ., 42, 4747-4754, doi: 10.1016/j.atmosenv.2008.01.042,
614 2008.
- 615 Li, L., Lollar, B. S., Li, H., Wortmann, U. G., Lacrampe-Couloume, G.: Ammonium stability and
616 nitrogen isotope fractionations for NH₄⁺-NH₃(aq)-NH₃ (gas) systems at 20–70 °C and pH of
617 2–13: applications to habitability and nitrogen cycling in low-temperature hydrothermal



- 618 systems. *Geochimica Et Cosmochimica Acta*, 84, 280-296. doi:10.1016/j.gca.2012.01.040.
619 2012.
- 620 Lobert, J. M., Scharffe, D. H., Hao, W. M., Crutzen, P. J.: Importance of biomass burning in the
621 atmospheric budgets of nitrogencontaining gases, *Nature*, 346, 552-554, 1990.
- 622 Michalski, G., Bhattacharya S. Girsch G.: NO_x cycle and the tropospheric ozone isotope anomaly:
623 an experimental investigation, *Atm. Chem. Phys.*, 14(10), 4935-4953, doi:
624 10.5194/acp-14-4935-2014, 2014.
- 625 Michalski, G., T. Meixner, M. Fenn, L. Hernandez, A. Sirulnik, E. Allen, and M. Thiemens.:
626 Tracing atmospheric nitrate deposition in a complex semiarid ecosystem using $\Delta^{17}\text{O}$,
627 *Environ.Sci.Technol.*, 38, 2175-2181, doi: 10.1021/es034980+, 2004.
- 628 Moore, H.: The isotopic composition of ammonia, nitrogen dioxide, and nitrate in the atmosphere,
629 *Atmos. Environ.*, 11, 1239-1243, 1977.
- 630 Pearson, J., Wells, D., Seller, K. J., Bennett, A., Soares, A., Woodall, J., Ingrouille, J.: Traffic
631 exposure increases natural ¹⁵N and heavy metal concentrations in mosses, *New Phytol.*, 147,
632 317-326, doi:10.1046/j.1469-8137.2000.00702.x, 2000.
- 633 Phillips, D. L. and Gregg, J. W.: Source partitioning using stable isotopes: coping with too many
634 sources, *Oecologia*, 136, 261-269, doi: 10.1007/s00442-003-1218-3, 2003.
- 635 Savarino, J., Morin, S., Erbland, J., Grannec, F., Patey, M. D., Vicars, W., Alexander, B.,
636 Achterberge, E. P.: Isotopic composition of atmospheric nitrate in a tropical marine boundary
637 layer, *Proc Natl Acad Sci USA*, 110(44), 17668-17673. doi/10.1073/pnas.1216639110. 2013.
- 638 Song, Y., Tang, X., Xie, S., Zhang, Y., Wei, Y., Zhang, M., Zeng, L., Lu, S.: Source
639 apportionment of PM_{2.5} in Beijing in 2004, *J. Hazard. Mater.*, 146, 124-130, doi:
640 10.1016/j.jhazmat.2006.11.058, 2007.
- 641 Sun, Y. L., Zhuang, G. S., Tang, A. H., Wang, Y., An, Z. S.: Chemical characteristics of PM_{2.5}
642 and PM₁₀ in haze-fog episodes in Beijing, *Environ. Sci. Technol.*, 40, 3148-3155, doi:
643 10.1021/es051533g, 2006.
- 644 Walters, W. W., Goodwin, S. R., Michalski, G.: The Nitrogen stable isotope composition (¹⁵N) of
645 vehicle emitted NO_x, *Environ. Sci. Technol.*, 49(4), 2278-2285, doi: 10.1021/es505580v,
646 2015.



- 647 Wang, C., Wang, X. B., Liu, D. W., Wu, H. H., Lu, X. T., Fang, Y. T., Cheng, W. X., Luo, W. T.,
648 Jiang, P., Shi, J. S., Yin, H. Q., Zhou, J. Z., Han, X. G., Bai, E.: Aridity threshold in
649 controlling ecosystem nitrogen cycling in arid and semi-arid grasslands, *Nature Commun.*, 5,
650 4799, DOI: 10.1038/ncomms5799, 2014.
- 651 Wang, D., Hu, J., Xu, Y., Lv, D., Xie, X., Kleeman, M., Xing, J., Zhang, H., Ying, Q.: Source
652 contributions to primary and secondary inorganic particulate matter during a severe
653 wintertime PM_{2.5} pollution episode in Xi'an, China, *Atmos. Environ.*, 97, 182-194, doi:
654 10.1016/j.atmosenv.2014.08.020, 2014.
- 655 Yeatman, S. G., Spokes, L. J., Dennis, P. F., Jickells, T. D.: Comparisons of aerosol nitrogen
656 isotopic composition at two polluted coastal sites, *Atmos. Environ.*, 35, 1307-1320, doi:
657 10.1016/S1352-2310(00)00408-8, 2001.
- 658 Yin, L., Niu, Z., Chen, X., Chen, J., Xu, L., Zhang, F.: Chemical compositions of PM_{2.5} aerosol
659 during haze periods in the mountainous city of Yong'an, China, *J. Environ. Sci.*, 24,
660 1225-1233, doi: 10.1016/51001-0742(11)60940-6, 2012.
- 661 Zhang, F., Xu, L., Chen, J., Chen, X., Niu, Z., Lei, T., Li, C., Zhao, J.: Chemical characteristics of
662 PM_{2.5} during haze episodes in the urban of Fuzhou, China, *Particuology*, 11, 264-272, doi:
663 10.1016/j.partic.2012.07.001, 2013.
- 664 Zhang, L., Wang, T., Lv, M. Y., Zhang, Q.: On the severe haze in Beijing during January 2013:
665 Unraveling the effects of meteorological anomalies with WRF-Chem, *Atmos. Environ.*, 104,
666 11-21, doi: 10.1016/j.atmosenv.2015.01.001,
- 667 Zhang, R. J., Jing, J., Tao, J., Hsu, S.-C., Wang, G., Cao, J. J., Lee, C. S. L., Zhu, L., Chen, Z.,
668 Zhao, Y., Shen, Z.: Chemical characterization and source apportionment of PM_{2.5} in Beijing:
669 seasonal perspective, *Atmos. Chem. Phys.*, 13, 7053-7074, doi: 10.5194/acp-13-7053-2013,
670 2013.
- 671 Zheng, M., Salmon, L. G., Schauer, J. J., Zeng, L., Kiang, C. S., Zhang, Y., Cass, G. R.: Seasonal
672 trends in PM_{2.5} source contributions in Beijing, China, *Atmos. Environ.*, 39, 3967-3976, doi:
673 10.1016/j.atmosenv.2005.03.036, 2005.
- 674
675



676 **Table 1.** Mass concentrations of inorganic N (IN, mainly including $\text{NH}_4^+\text{-N}$, $\text{NO}_3^-\text{-N}$),
 677 $\text{SO}_4^{2-}\text{-S}$, total N (TN), molecular ratios of NH_4^+ to NO_3^- , NH_4^+ to SO_4^{2-} , NH_4^+ to
 678 $(\text{NO}_3^- + \text{SO}_4^{2-})$ in $\text{PM}_{2.5}$ at Beijing (CRAES site) and a background site (Menyuan,
 679 Qinghai province) of China. Data of ambient NH_3 and SO_2 at Beijing site were cited
 680 from Carmichael et al (2003), He et al (2014), Wei et al (2015). Data of NH_3 and SO_2
 681 were cited from the background site of Waliguan in Qinghai Province (Carmichael et
 682 al., 2003).

	Beijing (CRAES site)	Menyuan, Qinghai
$\text{PM}_{2.5}$ ($\mu\text{g}/\text{m}^3$)	264.3 ± 118.0 (43.0–433.6)	13.0 ± 3.2 (7.0–17.8)
$\text{NH}_4^+\text{-N}$ (%)	7.4 ± 3.4 (3.5–12.9)	5.9 ± 1.8 (3.1–9.4)
$\text{NO}_3^-\text{-N}$ (%)	5.0 ± 3.0 (0.7–9.4)	1.9 ± 0.4 (1.2–2.6)
$\text{SO}_4^{2-}\text{-S}$ (%)	5.5 ± 2.4 (2.4–8.3)	0.2 ± 0.0 (0.2–0.3)
IN (%)	12.4 ± 4.6 (5.1–22.2)	7.8 ± 1.7 (5.7–11.3)
TN (%)	16.7 ± 4.6 (8.2–29.3)	8.6 ± 5.6 (1.4–18.7)
n- NH_4^+ /n- NO_3^-	2.5 ± 2.5 (0.5–9.0)	3.3 ± 1.2 (1.2–4.9)
n- NH_4^+ /n- SO_4^{2-}	3.5 ± 1.6 (1.2–6.3)	56.3 ± 14.3 (42.1–89.5)
n- NH_4^+ /n- $(\text{NO}_3^- + \text{SO}_4^{2-})$	1.1 ± 0.6 (0.4–2.9)	3.1 ± 1.1 (1.2–4.7)
n- NH_4^+ /n- $(\text{NO}_3^- + 1/2 * \text{SO}_4^{2-})$	1.4 ± 1.0 (0.5–4.3)	3.2 ± 1.2 (1.2–4.8)
NH_3 ($\mu\text{g}/\text{m}^3$)	14.1	4.8
NO_2 ($\mu\text{g}/\text{m}^3$)	89.2 ± 21.2 (57.0–122.0)	4.3 ± 1.3 (2.6–6.7)
SO_2 ($\mu\text{g}/\text{m}^3$)	22.9	0.3
n- NH_3 /n- NO_2	0.4	3.0
n- NH_3 /n- SO_2	2.3	60.2
n- NH_3 /n- $(\text{NO}_2 + \text{SO}_2)$	0.4	2.9
n- NH_3 /n- $(\text{NO}_2 + 1/2 * \text{SO}_2)$	0.4	2.9

683

684

685

686

687



688 **Table 2.** Fractional contributions (f , %) of dominant N precursors and anthropogenic
 689 N sources to N in $PM_{2.5}$ at Beijing (CRAES site) and a background site (Menyuan,
 690 Qinghai province) of China.

Site	Precursor		f_{NH_3}/f_{NO_2}	Anthropogenic source		
	f_{NH_3}	f_{NO_2}		$f_{industrial}$	$f_{traffic}$	$f_{agricultural}$
Beijing	44±20	41±19	1.5±1.1	41±18	30±12	
Menyuan	61±11	27±8	2.3±1.1			82±7 58±9

691

692

693

694

695

696

697

698

699

700

701

702

703

704

705

706

707

708



709 **Figure captions**

710 **Fig. 1.** $\delta^{15}\text{N}$ values of $\text{PM}_{2.5}$ and potentially dominant N sources at Beijing (CRAES
711 site) (red) and a background site (Menyuan, Qinghai province) (blue) of China,
712 respectively. The solid and dotted lines within the boxes mark the arithmetic mean and
713 median values, respectively. Source $\delta^{15}\text{N}$ data (detailed in Table S2) were cited from
714 Moore, 1974, 1977; Heaton, 1986; Heaton, 1990; Freyer, 1991; Kiga et al., 2000;
715 Laffray et al., 2000; Heaton et al., 2004; Li & Wang, 2008; Elliott et al., 2009;
716 Hastings et al., 2009; Kawashima & Kurahashi, 2011; Middlecamp & Elliot, 2011;
717 Felix et al., 2012, 2013, 2014; Felix & Elliott, 2014; Walters et al., 2015. The $\delta^{15}\text{N}$ of
718 TN in soil (Wang et al., 2014) was assumed as TN of soil dust according to the air
719 mass backward trajectories (Fig. 2).

720 **Fig. 2.** 72-hour air mass backward trajectories for all sampling dates at Beijing and a
721 background site (Menyuan, Qinghai Province) of China, based on NOAA HYSPLIT
722 model back trajectories.

723 **Fig. 3** Correlation between $\delta^{15}\text{N}$ values of $\text{PM}_{2.5}$ and molecular ratios of NH_4^+ to
724 $(\text{NO}_3^- + 1/2*\text{SO}_4^{2-})$ ($n\text{-NH}_4^+/n\text{-}(\text{NO}_3^- + 1/2*\text{SO}_4^{2-})$) in $\text{PM}_{2.5}$ at Beijing (CRAES site)
725 and a background site (Menyuan, Qinghai province) of China.

726 **Fig. 4.** Fractional contributions (f , %) of dominant N sources to N in $\text{PM}_{2.5}$ at Beijing
727 (CRAES site) (red) and a background site (Menyuan, Qinghai province) (blue) of
728 China, respectively. The solid and dotted lines within the boxes mark the median and
729 the mean values. The mean percentage calculated by the IsoSource model was taken
730 as the fractional contribution of each source to TN of each $\text{PM}_{2.5}$ sample.

731

732



733 **Figure 1**

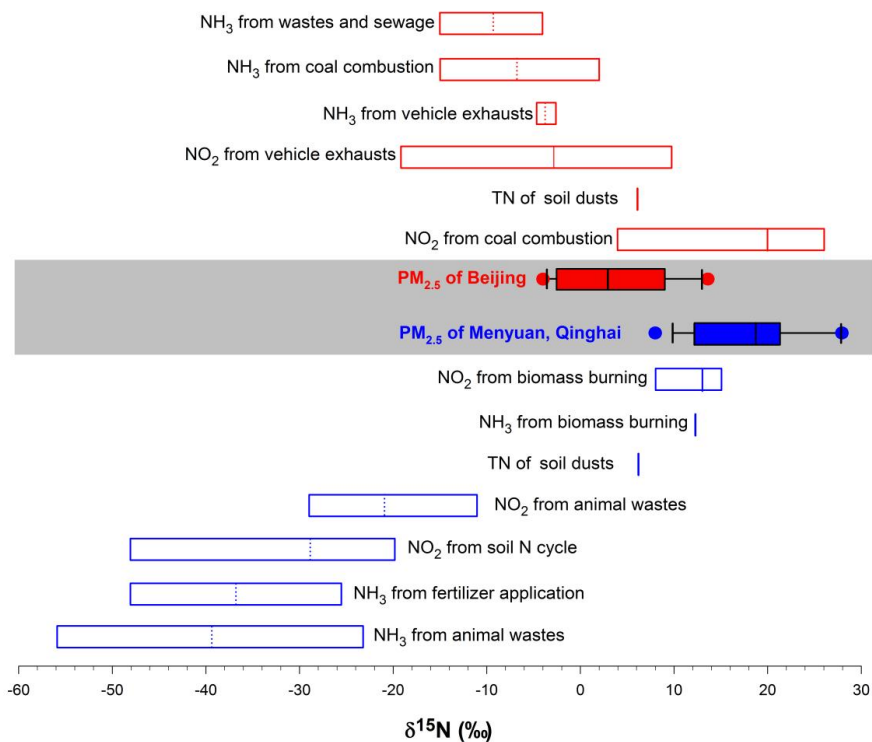
734

735

736

737

738



739

740

741

742

743

744



745 **Figure 2**

746

747

748

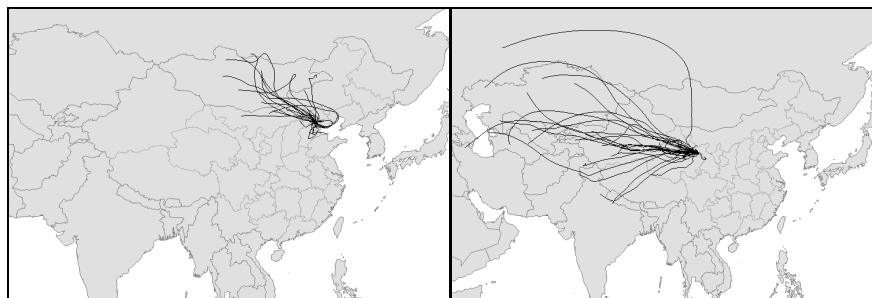
749

750

751

752

753



754

755

756

757

758

759

760

761

762

763

764

765



766 **Figure 3**

767

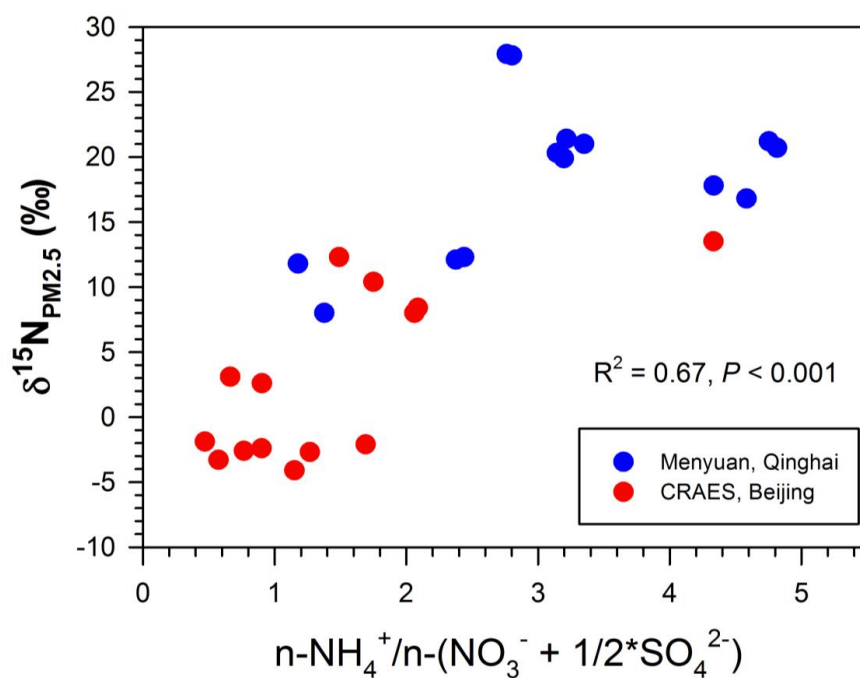
768

769

770

771

772



773

774

775

776

777

778

779



780 **Figure 4**

781

782

783

784

